ANNALS OF FACULTY ENGINEERING HUNEDOARA
– INTERNATIONAL JOURNAL OF ENGINEERING
Tome X (Year 2012) – FASCICULE 3 (ISSN 1584 – 2673)

[1.] Mirela C. GHIȚĂ, [2.] Anton C. MICU, [3.] Mihai D.L. ȚĂLU, [4.] Ştefan D.L. ȚĂLU

SHAPE OPTIMIZATION OF VEHICLE'S METHANE GAS TANK

[1.] "SPIRU HARET" UNIVERSITY OF CRAIOVA, FACULTY OF MANAGEMENT, ROMANIA
[2.] UNIVERSITY POLITEHNICA OF BUCHAREST, FACULTY OF MECHANICAL ENGINEERING AND MECHATRONICS, ROMANIA
[3.] UNIVERSITY OF CRAIOVA, FACULTY OF MECHANICAL ENGINEERING, DEPARTMENT OF APPLIED MECHANICS, ROMANIA
[4.] TECHNICAL UNIVERSITY OF CLUJ-NAPOCA, FACULTY OF MECHANICAL ENGINEERING, DEPARTMENT OF AUTOMOTIVE ENGINEERING AND TRANSPORTATION, ROMANIA

ABSTRACT: *The objective of this paper is to present a method that allows the optimal design of the steel gas tank used in the automotive industry for storage of the methane gas based on the application of the Finite Element Method (FEM). The engineering design of the gas tank is performed using a specialized database of 3D parameterized shapes.*
KEYWORDS: *engineering design, methane gas tank, optimization, Finite Element Method*

INTRODUCTION

One alternative to fossil combustibles used to modern automotive engines is CH_4 gas, an applied solution ever since the early part of the 20th century [1].

The major disadvantage of this solution was caused by vehicle's low autonomy, due to reduced volume of CH_4 gas which could be stored in the tank, accompanied by the explosion risk disadvantage. On the other hand, the main advantage of this solution was offered by a running lower cost per kilometer comparative to that of gasoline or diesel oil.

Figure 1 shows two equipping solutions of an Opel Zafira 1.6 CNG Turbo model car with CH_4 gas tanks, connected in parallel and disposed on the lower panel and in the car trunk. It is the first CNG turbo-charged vehicle in this segment with a top speed of 200 km/h. In this case, the cost of running on natural gas is about 50 percent less than a comparable petrol model. Additionally, the Zafira 1.6 CNG Turbo can run on both natural gas/bio-methane and regular gasoline [2].

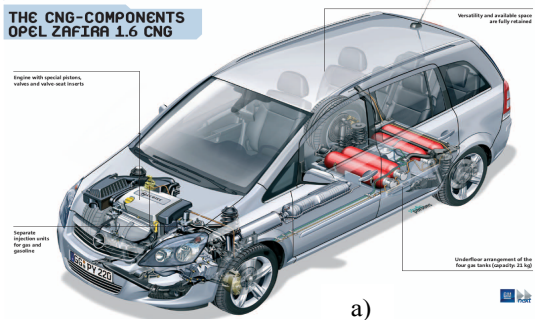

a)

b)

Figure 1. Equipping solutions of an Opel Zafira 1.6 CNG Turbo model car with CH_4 gas tanks, connected in parallel and disposed: a) on the lower panel; b) in the car trunk [2]

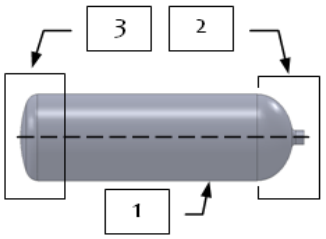

Figure 2. A shape for the gas tank cover

As a principle, a CH_4 gas tank for automotive industry is made of three elements: a lateral one - 1, an end up one - 2 and a bottom one - 3, as shown in Figure 2. Usually, elements 1 or 2 have a socket where the filling-emptying tap is mounted.

Due to the wide variety of these gas tank covers, their design optimization is done separately (Figure 3). Elements are assembled afterwards to get the final form of the gas tank cover.

In engineering design, the optimized dimensions are afterwards rounded up to real values. A new analysis of efforts and deformation states is done afterwards and the surety coefficient value is calculated and compared with the admissible value.

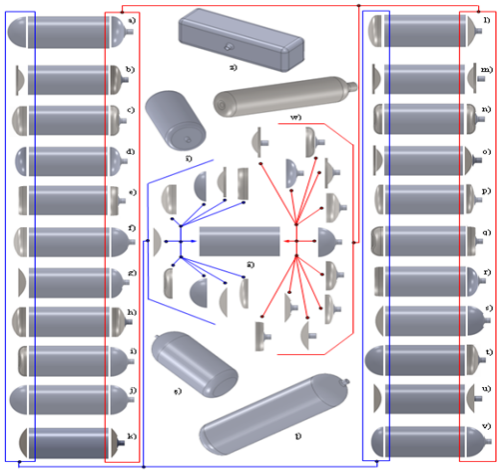

Figure 3. Different constructive shapes for the gas tank cover

The mechanical simulation, numerical calculations and geometrical modeling are a complex task, especially for the three-dimensional models [3-21].

THE PROPOSED METHOD FOR OPTIMIZATION

This paper proposes a method to optimize CH_4 gas tanks for automotive industry, based on a specialized database of 3D parameterized shapes, involving the use of the Finite Element Method [22, 23]. The optimization method includes the following steps:

- *the shape of the gas tank is chosen from the Figure 3;*
- *the shape is decomposed into its main components and the type of gas tank cover is identified;*
- *the gas tank covers are selected from the specialized database of 3D parameterized shapes;*
- *the material selected for the construction of the gas tank covers is chosen;*
- *the shape and dimensions of the gas tank covers are modelled and optimized using the FEM;*
- *the real dimensions of the gas tank covers are rounded to the nearest representable values;*
- *the 3D parameterized real model of the gas tank is modelled and assembled;*
- *a study of efforts and deformation states is performed using the 3D real assembly model.*

DIMENSIONAL OPTIMIZATION OF THE GAS TANK USING THE FEM

The optimum design through the Finite Elements Method can significantly reduce the weight, the cost of manufacturing and increase security and even the reliability of the gas tank.

The proposed method is applied to determine the optimal shape of a gas tank for automotive industry, designated to storage CH_4 gas, made from stainless steel.

The gas tank is made up from a cylindrical lateral cover and two end up covers: one has a torispherical shape and the other one has a hemispherical shape, penetrated.

THE OPTIMIZATION OF THE CYLINDRICAL LATERAL SHAPE OF THE GAS TANK COVER

For mathematical calculations, we use next input data:

- *the maximum test pressure: p_h = 30 N/mm^2;*
- *the normal range of working temperature: T = -20 ^{o}C,..., +60 ^{o}C;*
- *the type of gas tank cover material: AISI 4340;*
- *the value of gas tank cover diameter: ϕ = 200 mm.*

The optimization of the cylindrical lateral shape of the gas tank cover has the purpose to obtain a minimum mass and a normal unit resultant effort lower than the admissible one: $\sigma_{rez\ efectiv} \leq \sigma_a$.

Because the gas tank cover has an axial constructive symmetry (Figure 4) and a symmetric loading under-pressure on the inner axial symmetric surface, the optimization can be done on a 1/4 part of the initial model (Figure 5), to which are applied accordingly: the distributed force loads, the local material connections and the conditions of symmetry on the contour (Figure 6).

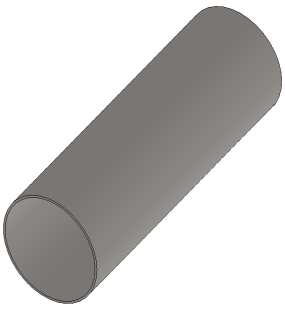

Figure 4. The lateral cylindrical cover

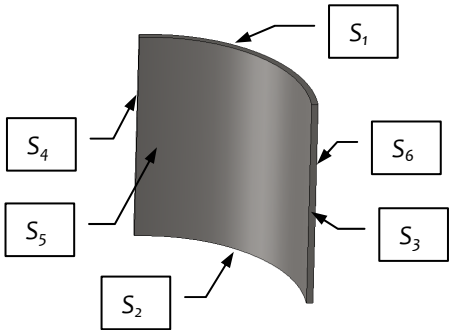

Figure 5. A 1/4 model of the initial lateral cylindrical cover

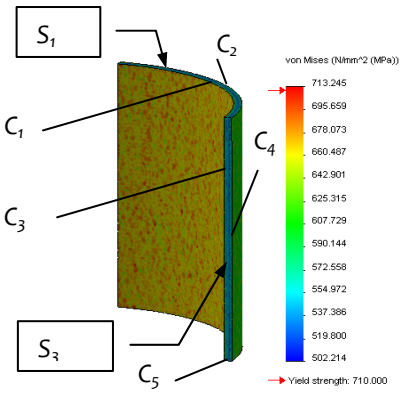

Figure 6. The resultant effort von Mises for optimal solution

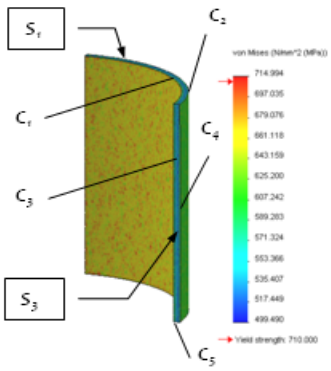

Figure 7. The resultant effort von Mises for real solution

The restrictions of constructive symmetry are applied on the surfaces S_1,..., S_4 (Figure 6). The distributed force loads that are applied on the cover are:

- *the pressure p_h = 30 N/mm^2 on surface S_5 and the atmospheric one on outer surface S_6;*
- *the thermal loads on surfaces S_5 and S_6, with T = -20 ^{o}C,..., +60 ^{o}C;*
- *the opposite forces $F_{p1} = F_{p2} = p_h (\pi D_e^2/4)/4$ = 235612 N, on surfaces S_1 and S_2, due to the pressure on the inner surfaces of end up covers.*

The considered variable within the optimization process is the cover thickness s. Applying the SolidWorks 2011 software to the 3D model, we get the results shown in Table 1. These results reveal an optimal thickness of the wall of s_o = 4.58 mm and a maximal resultant effort von Mises of $\sigma_o\ /_{T=-20\ C}$ = 709.87 N/mm^2 (Figure 6), lower than the value σ_a= 710 N/mm^2.

Once the real thickness of the wall s = 4.6 mm was chosen, with the FEM is analyzed (Figure 7) the real effort variation $\sigma_r(T)\,/_{s\,=\,4.6\ mm}$ and the obtained values from the Table 1 show a maximal deviation of $\Delta\sigma$ = - 0.46 %, calculated with next relation: $\Delta\sigma[\%] = (\sigma_r - \sigma_o)/\sigma_o \cdot 100$.

Table 1: The optimized results obtained by applying the SolidWorks 2011 software to the 3D model

No.	T [°C]	σ_o [N/mm²]	σ_r [N/mm²]	$\Delta\sigma$	No.	T [°C]	σ_o [N/mm²]	σ_r [N/mm²]	$\Delta\sigma$
1	-20	709.87	705.870	-0.563	10	25	590.762	588.211	-0.424
2	-15	698.972	700.503	0.219	11	30	587.937	585.440	-0.379
3	-10	684.831	686.114	0.187	12	35	591.470	589.227	-0.448
4	-5	670.836	671.782	0.141	13	40	597.337	594.658	-0.454
5	0	657.005	657.564	0.085	14	45	602.840	600.102	-0.460
6	5	643.328	643.420	0.014	15	50	608.358	605.556	-0.442
7	10	629.837	629.375	-0.073	16	55	613.888	611.174	-0.356
8	15	616.515	615.444	-0.173	17	60	619.466	617.259	-0.424
9	20	603.386	601.621	-0.292					

The variation law $\sigma_r(T)$ obtained by interpolation with the least-squares method is:

$$\sigma_r(T) = 654.5852668 - 2.828971715 \cdot T + 0.011197002 \cdot T^2 + 0.0004637323 \cdot T^3 \quad (1)$$

For the real cover, the spatial distribution of effort $\sigma_r(T)$ is given in Figure 7, while its variation on curves C_1, .., C_5 is shown in Figure 8 to Figure 12.

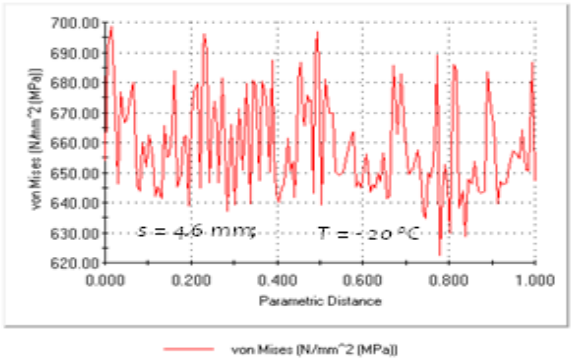

Figure 8. The effort variation $\sigma_r(T)$ on curve C_1
On curve C_1: σ_{min} = 622.44 N/mm², σ_{med}= 659.28 N/mm², σ_{max}= 698.50 N/mm²

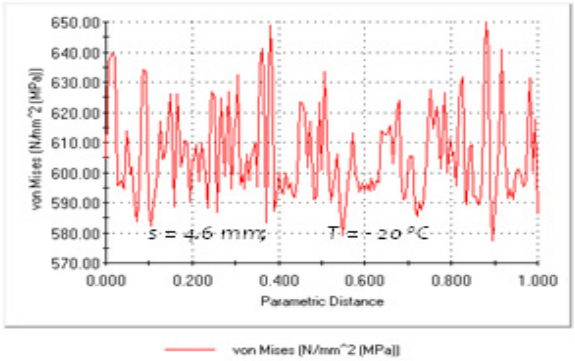

Figure 9. The effort variation $\sigma_r(T)$ on curve C_2
On curve C_2: σ_{min} = 577.21 N/mm², σ_{med}= 605.81 N/mm², σ_{max}= 650.00 N/mm²

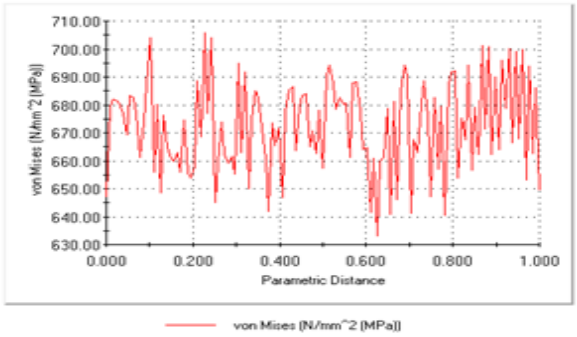

Figure 10. The effort variation $\sigma_r(T)$ on curve C_3
On curve C_3: σ_{min} = 633.29 N/mm²,
σ_{med}= 672.56 N/mm², σ_{max}= 705.87 N/mm²

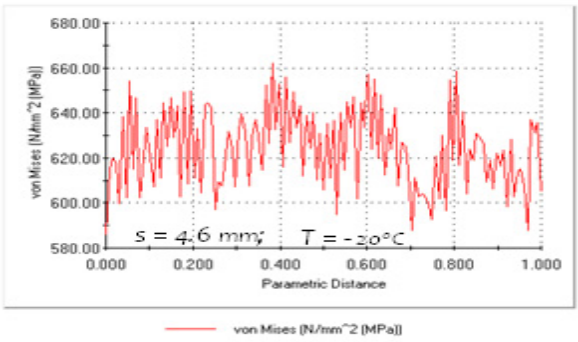

Figure 11. The effort variation $\sigma_r(T)$ on curve C_4
On curve C_4: σ_{min} = 586.23 N/mm²,
σ_{med}= 623.98 N/mm², σ_{max}= 662.16 N/mm²

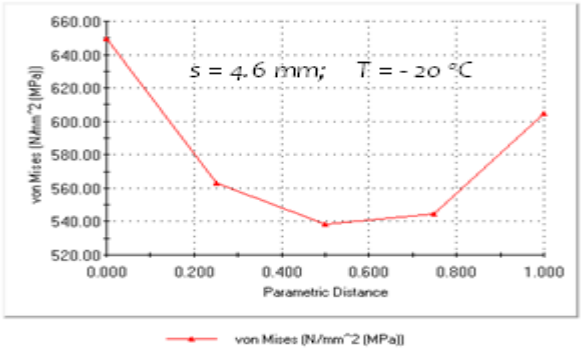

Figure 12. The effort variation $\sigma_r(T)$ on curve C_5
On curve C_5: σ_{min} = 538.61 N/mm²:
σ_{med}= 580.10 N/mm²: σ_{max}= 649.40 N/mm²

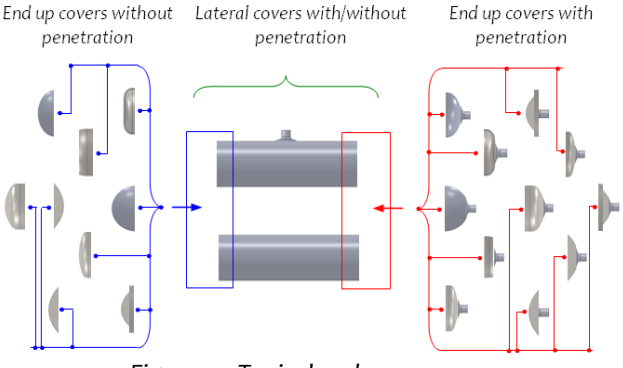

Figure 13. Typical end up covers

THE OPTIMIZATION OF THE TANK'S END UP COVERS

In practice, a variety of constructive forms for simple or composed end up covers are used to manufacture the low or high pressure automotive gas tanks.

Figure 13 shows some types of constructive shapes for end up covers.

THE OPTIMIZATION OF TOROSPHERIC END UP COVER WITHOUT PENETRATION

In this case, the input data used for optimization are identical with those of the lateral cover, to which is supplementary applied the condition of having the equality between the lid diameter and the cover diameter.

The 3D modeling of torospheric cover is given in Figure 14, a, and a detail A (Figure 14, b).

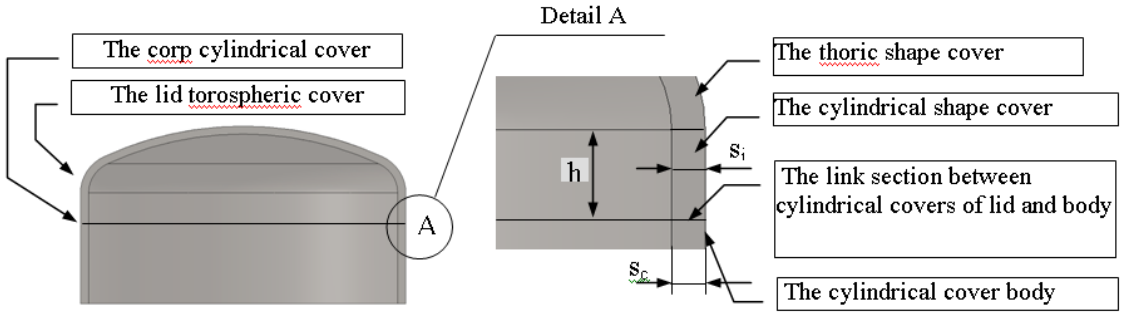

Figure 14. The 3D modelling of: a) the torospheric cover and b) a detail A

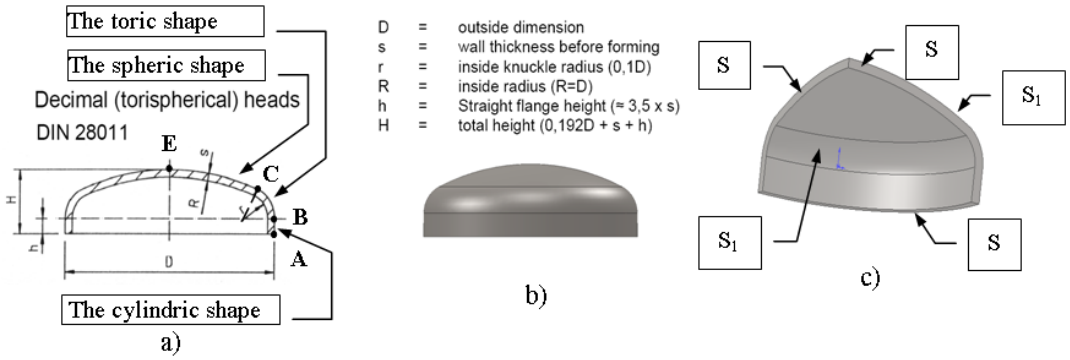

Figure 15. The 3D design of the torospheric cover: a) the decimal (torispherical) heads according DIN 28011; b) the 3D model; c) a ¼ part of the 3D model

From DIN 28011 (Figure 15, a) are obtained the preliminary calculation formulae that determine the dimensions from Table 2 for diameter D = 200 mm of a torospheric, unpenetrated shape cover.

Table 2: The calculus formulae of constructive dimensions for the case of torospheric unpenetrated shape cover with diameter D = 200 mm

D	s_c	s_i	r	R	h	H
		$\geq 1.5\ s_p$	0.1 D	D	$\cong 3.5\ s$	0.192 D + s+ h
These dimensional values are preliminary indicated [mm]						
200	5	7.5	20	200	17.5	60.9
These dimensional values are accepted as initial data for optimization calculus [mm]						
200	5	8	20	200	20	62

As in the case of the lateral cover, the torospheric cover shows an axial constructive symmetry and an axial symmetric loading. Therefore, the optimization study is performed on a ¼ part of the initial model, to which are applied accordingly: the distributed force loads, the local material connections and the conditions of symmetry on the contour.

The symmetry restrictions are applied on surfaces: S_7 and S_8, and for the normal movement cancelation on the surface S_9.

The distributed force loads applied to the torospheric cover are: the pressure p_h = 30 N/mm^2 on the inner surface S_{10}, and the atmospheric one on the outer surface S_{11}; the thermal loads on the surfaces S_{10} and S_{11}, with T = -20 ^{o}C, ..., +60 ^{o}C;

The variables for optimization are: the thickness s, the total height H and the height of the cylindrical cover h. The obtained results within the optimization process are shown in Tabel 3.

Table 3: The optimized results for a torospheric un-penetrated shape cover with the diameter D = 200 mm

[mm]	s_i	R	h	H
The optimal value	4.96	130	6.2	72.01
The real values accepted	5	130	6	72

The variation of the real resultant effort von Mises σ_r (T) is given in Tabel 4.

Table 4: The variation of the real resultant effort von Mises σ_r (T)

No.	T [°C]	σ_r [N/mm^2]	No.	T [°C]	σ_r [N/mm^2]
1	-20	694.441	10	25	590.791
2	-15	681.997	11	30	584.078
3	-10	669.718	12	35	581.115
4	-5	657.618	13	40	578.259
5	0	645.705	14	45	575.510
6	5	633.990	15	50	572.870
7	10	622.485	16	55	570.342
8	15	611.201	17	60	567.926
9	20	600.690			

The variation law $\sigma_r(T)$ obtained by interpolation with the least-squares method is:

$$\sigma(T) = 644.23063 - 2.379359916 \cdot T + 0.01224435501 \cdot T^2 + 0.0001171706226 \cdot T^3 \quad (2)$$

It can be seen that the real state of spatial distribution has a maximum value of σ_r = 694.44 N/mm^2 for T = -20 °C (Figure 16) and the maximum linear deformation resultant is u_r = 0.328 mm for T = 60 °C (Figure 17).

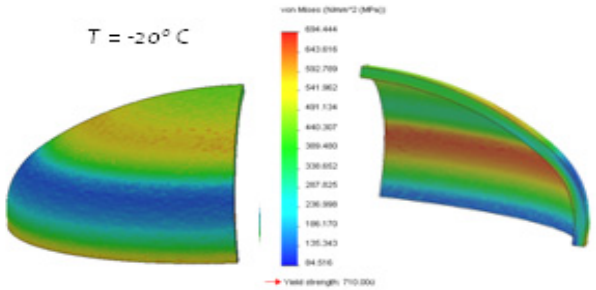

Figure 16. The spatial von Mises distribution

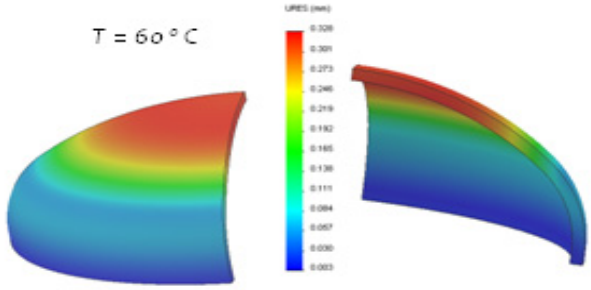

Figure 17. The spatial linear deformation distribution

The relation between the σ_{ph} [N/mm^2] and u_{ph} [mm] with the temperature variation is shown in Tabel 5.

Table 5: The relation between the σ_{ph} [N/mm^2] and u_{ph} [mm] with the temperature variation

No.	T [°C]	σ_{ph} [N/mm^2]	u_{ph} [mm]	No.	T [°C]	σ_{ph} [N/mm^2]	u_{ph} [mm]
1	-20	694.441	0.32131	10	25	590.791	0.32471
2	-15	681.997	0.32169	11	30	584.078	0.32512
3	-10	669.718	0.32206	12	35	581.115	0.32553
4	-5	657.618	0.32244	13	40	578.259	0.32594
5	0	645.705	0.32281	14	45	575.510	0.32635
6	5	633.990	0.32319	15	50	572.870	0.32676
7	10	622.485	0.32357	16	55	570.342	0.32717
8	15	611.201	0.32395	17	60	567.926	0.32759
9	20	600.690	0.32433				

THE OPTIMIZATION OF HEMISPHERIC END UP COVER WITH PENETRATION

The input data are the same as for end up cover without penetration and the spatial shaping is given in Figure 18, based on geometric dimensions from the Tabel 6.

Table 6: The geometric dimensions

D [mm]	r_1 [mm]	r_2 [mm]	H = D/2 [mm]	h [mm]	d [mm]	s [mm]
200	10	14	100	20	20	4.5

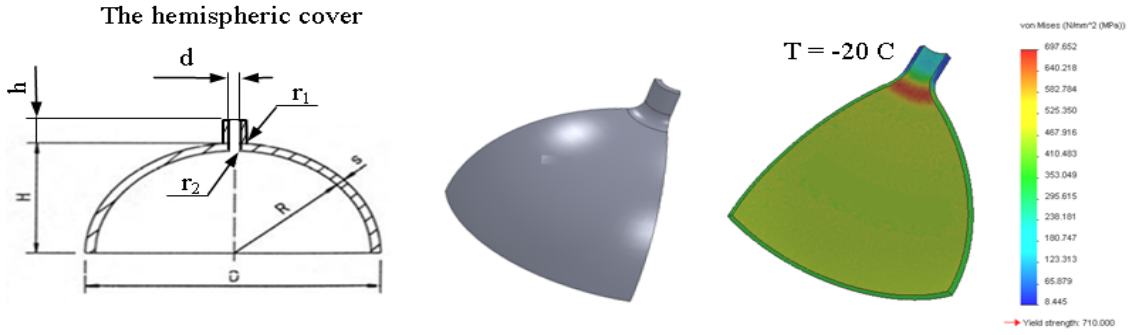

Figure 18. The 3D design of the hemispheric end up cover with penetration: a) the 2D representation; b) a ¼ part of the 3D model; c) the FEM applied to a ¼ part of the 3D model

In this case, the cover shows an axial constructive symmetry and an axial symmetric loading of the inner surface.

The optimization study was performed on an equivalent model obtained through the sectioning of a ¼ from the initial model (Figure 18, b). The symmetry contour restrictions were applied on the corresponding surfaces. The distributed force loads for the cover are the same as for the cover without penetration. The optimized variable was the thickness of the cover s.

After simulation with the FEM, for an optimal thickness s_o = 3.93 mm is obtained a resultant effort von Mises $\sigma_o\,/_{ph=30N/mm2;\ T=-20C}$ = 708.35 N/mm².

Considering a real thickness of the cover s = 4 mm, the 3D variation of the real effort von Mises σ_r (T) (Figure 18, c) and the linear deformation resultant are shown in Tabel 7.

Table 7: The variation of the resultant effort von Mises σ_r (T) and the resultant linear deformation

No.	T[°C]	σ_r [N/mm²]	u_r [mm]	No.	T[°C]	σ_r [N/mm²]	u_r [mm]
		p_h = 30 N/mm²				p_h = 30 N/mm²	
1	-20	697.652	0.12922	10	25	612.080	0.13547
2	-15	687.622	0.12991	11	30	609.139	0.13624
3	-10	677.706	0.13061	12	35	610.711	0.13702
4	-5	667.909	0.13130	13	40	612.366	0.13780
5	0	658.236	0.13199	14	45	614.104	0.13859
6	5	648.693	0.13268	15	50	615.923	0.13938
7	10	639.286	0.13338	16	55	617.823	0.14017
8	15	630.021	0.13407	17	60	619.803	0.14095
9	20	620.904	0.13476				

The corresponding variation laws of the effort and deformation, obtained by interpolation based on the data from Table 7, with the least-squares method are:

$$\sigma_{ph}(T) = 656.30315 - 1.97727383 \cdot T + 0.012441134 \cdot T^2 + 0.00019265 \cdot T^3 \quad (3)$$

$$u_{ph}(T) = 0.13197095 + 0.000138 \cdot T + 0.113364 \cdot 10^{-6} \cdot T^2 + 0.14379 \cdot 10^{-8} \cdot T^3 \quad (4)$$

THE FINITE ELEMENT ANALYSIS OF THE REAL GAS TANK

The 3D model of the gas tank is based on the previous determined parts with real dimensions. The requirements of the finite element analysis for the gas tank are identical to those applied in the optimization process of components, previously mentioned.

As a result of the finite element analysis, the spatial distributions of the resultant efforts state von Mises and of the linear deformations are shown in Figure 19 (the view on inner surface of the gas tank) and Figure 20 (the view on outer surface of the gas tank).

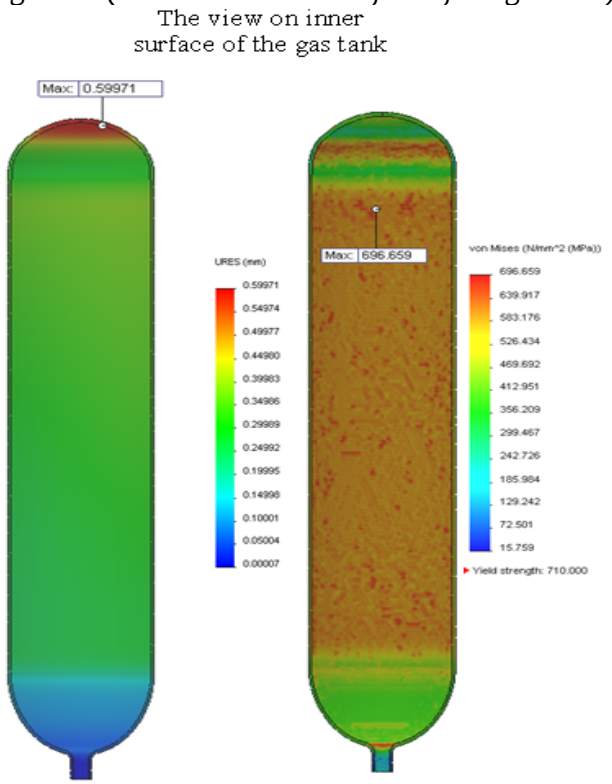

Figure 19. The spatial distributions of the resultant efforts state von Mises and of the linear deformations (the view on inner surface of the gas tank)

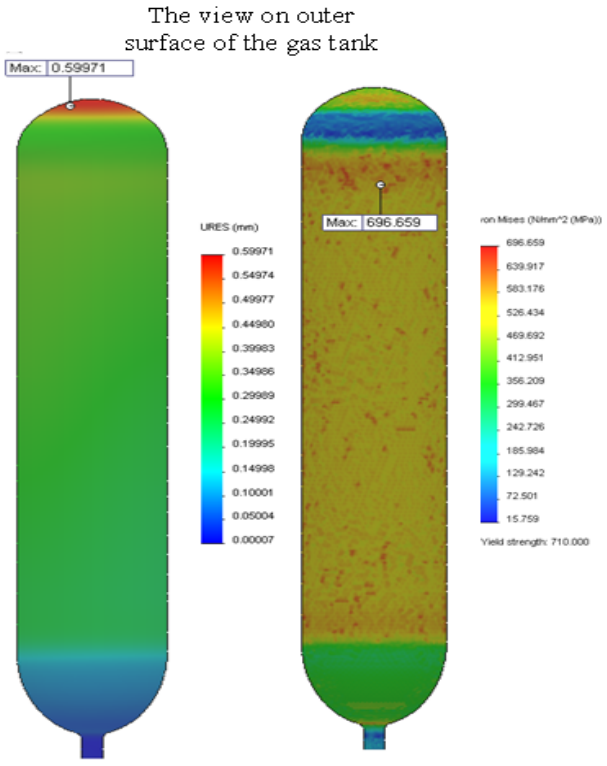

Figure 20. The spatial distributions of the resultant efforts state von Mises and of the linear deformations (the view on outer surface of the gas tank)

For the most exposed zones of gas tank covers, the effort von Mises resultant is lower than the admissible value, $\sigma_a = 710$ N/mm^2.

CONCLUSIONS

For the optimization of the cylindrical lateral shape of the gas tank cover, the maximal real solicitation is of $\sigma_r /_{T=-20\,C} = 709.87$ N/mm^2, with 0.0183 % lower than the admissible effort σ_a.

There is an increase of the metal used mass with $\Delta m = 0.4366$ %, when it is made the rounding of thickness for the real lateral cover.

Based on the data from Table 1, it can be noticed that for the range temperature T = -20 ^oC, ..., 30^oC, the resultant real effort decreases from the value $\sigma_r /_{T=-20\,C} = 705.87$ N/mm^2 to $\sigma_r /_{T=30\,C} = 585.44$ N/mm^2, and after that it increases to the value of $\sigma_r /_{T=60\,C} = 617.259$ N/mm^2

The real effort σ_r deviation relative to the optimal effort σ_o, for the range temperature T = -15 ^oC,...,5 ^oC, is positive, with a maximum value of $\Delta\sigma = 0.219$ %, reached at T = -15 ^oC, while for the other temperature values in the negative field, it reaches a minimum of $\Delta\sigma = -0.563$ %, for a temperature T = -20 ^oC.

For the case of torospheric end up cover without penetration, on T = - 20 ^oC it appears the effort maximal von Mises on the inner surface of the cover, being of $\sigma_r = 694.441$ N/mm$^2 \leq \sigma_a = 710$ N/mm^2.

For the case of hemispheric end up cover with penetration, the resultant linear deformation state $u_r = 0.14095$ mm is maximal on T = 60 ^oC, while von Mises effort state is $\sigma_r = 697.65$ N/mm^2 on T = -20 ^oC. In the case of 3D real tank, the finite element analysis shows the maximum values $\sigma_{r\ max} = 696.659$ N/mm^2 and $u_{r\,max} = 0.59971$ mm.

Based on these results, it can be seen that the proposed method for dimensional optimization applied to the 3D parameterized components is correct and efficient.

The following acceptance tests were performed prior to delivery for methane gas tank:

a) preliminary examination;
b) pre-proof volumetric capacity;
c) ambient proof pressure;
d) post-proof volumetric capacity;
e) external leakage;
f) final examination;
g) cleanliness measurement.

REFERENCES

[1.] Shr-Hung, C., Master's Thesis: Novel design and optimization of vehicle's natural gas fuel tank, Ohio University, USA, 1997.
[2.] http://www.opel.com/ (accessed 10 June 2012)
[3.] Benton, J., Ballinger, I., Ferretti, A., Ierardo, N., Design and manufacture of a high performance, high mass efficient gas tank for the VEGA AVUM, AIAA-2007-5500, pp. 1-14.
[4.] Bîrleanu, C., Țălu, Ş., Organe de maşini. Proiectare şi reprezentare grafică asistată de calculator, Editura Victor Melenti, Cluj-Napoca, 2001.
[5.] Țălu, Ş., Limbajul de programare AutoLISP. Teorie şi aplicaţii, Editura Risoprint, Cluj-Napoca, 2001.
[6.] Țălu, Ş., Reprezentări grafice asistate de calculator, Editura Osama, Cluj-Napoca, 2001.
[7.] Țălu, Ş., Grafică tehnică asistată de calculator, Editura Victor Melenti, Cluj-Napoca, 2001.
[8.] Nițulescu, T., Țălu, Ş., Aplicaţii ale geometriei descriptive şi graficii asistate de calculator în desenul industrial, Editura Risoprint, Cluj-Napoca, 2001.
[9.] Dumitru, N., Margine, A., Organe de maşini. Asamblări. Elemente elastice. Proiectare asistată de calculator. Editura Universitaria, Craiova, 2002.
[10.] Dumitru, N., Margine, A., Bazele modelării în ingineria mecanică, Editura Universitaria, Craiova, 2002.
[11.] Țălu, Ş., AutoCAD 2005, Editura Risoprint, Cluj-Napoca, 2005.
[12.] Florescu-Gligore, A., Țălu, Ş., Noveanu, D., Reprezentarea şi vizualizarea formelor geometrice în desenul industrial, Editura U. T. Pres, Cluj-Napoca, 2006.
[13.] Țălu, Ş., Țălu, M., AutoCAD 2006. Proiectare tridimensională, Editura MEGA, Cluj-Napoca, 2007.
[14.] Țălu, Ş., Racocea C., Reprezentări axonometrice cu aplicaţii în tehnică, Editura MEGA, Cluj-Napoca, 2007.
[15.] Țălu, Ş., Geometrie descriptivă, Editura Risoprint, Cluj-Napoca, 2010.
[16.] Țălu, Ş., Țălu, M., A CAD study on generating of 2D supershapes in different coordinate systems, ANNALS of Faculty of Engineering Hunedoara - International Journal of Engineering, Hunedoara, Tomul VIII, Fasc. 3, 2010, pp. 201-203.
[17.] Țălu, Ş., Țălu, M., CAD generating of 3D supershapes in different coordinate systems., ANNALS of Faculty of Engineering Hunedoara - International Journal of Engineering, Hunedoara, Tomul VIII, Fasc. 3, 2010, pp. 215-219.
[18.] Racocea, C., Țălu, Ş., Reprezentarea formelor geometrice tehnice în axonometrie, Editura Napoca Star, Cluj-Napoca, 2011.

[19.] Țălu, Ș., Study on the construction of complex 3D shapes with superellipsoids and supertoroids, ANNALS of Faculty of Engineering Hunedoara - International Journal of Engineering, Hunedoara, Tomul IX, Fasc. 3, 2011, pp. 299-302.
[20.] Țălu, Ș., CAD representations of 3D shapes with superellipsoids and convex polyhedrons, ANNALS of Faculty of Engineering Hunedoara - International Journal of Engineering, Hunedoara, Tomul IX, Fasc. 3, 2011, pp. 349-352.
[21.] Țălu, Ș., Complex 3D shapes with superellipsoids, supertoroids and convex polyhedrons, Journal of Engineering Studies and Research, Bacău, vol. 17, nr. 4, 2011, pp. 96-100.
[22.] Fenner, R., Finite Element Methods For Engineers, Imperial College Press, 2nd Edition, UK, 2012
[23.] SolidWorks 3D CAD Design, User Guide, SolidWorks Corporation, 2011.

ANNALS OF FACULTY ENGINEERING HUNEDOARA
– INTERNATIONAL JOURNAL OF ENGINEERING